

# Anterior vs. posterior position of dispersive patch during radiofrequency catheter ablation: insights from *in silico* modelling

Ramiro M. Irastorza <sup>1,2†</sup>, Timothy Maher <sup>3†</sup>, Michael Barkagan <sup>4</sup>,  
Rokas Liubasuskas <sup>5</sup>, Enrique Berjano <sup>6</sup>, and Andre d'Avila <sup>3\*</sup>

<sup>1</sup>Instituto de Física de Líquidos y Sistemas Biológicos (CONICET), La Plata, Argentina; <sup>2</sup>Departamento de Ingeniería Mecánica, Facultad Regional La Plata, Universidad Tecnológica Nacional, La Plata, Argentina; <sup>3</sup>Division of Cardiovascular Medicine, Harvard-Thorndike Electrophysiology Institute, Beth Israel Deaconess Medical Center, Harvard Medical School, 330 Brookline Ave, Boston, MA 02215, USA; <sup>4</sup>Cardiology Division, Shamir Medical Center, Sackler school of Medicine, Tel Aviv University, Beer-Yakov, Israel; <sup>5</sup>Department of Medicine, Salem Hospital, Tufts University School of Medicine, Salem, MA, USA; and <sup>6</sup>BioMIT, Department of Electronic Engineering, Universitat Politècnica de València, Valencia, Spain

Received 17 August 2022; accepted after revision 16 December 2022; online publish-ahead-of-print 13 January 2023

## Aims

To test the hypothesis that the dispersive patch (DP) location does not significantly affect the current distribution around the catheter tip during radiofrequency catheter ablation (RFCA) but may affect lesions size through differences in impedance due to factors far from the catheter tip.

## Methods

An *in silico* model of RFCA in the posterior left atrium and anterior right ventricle was created using anatomic measurements from patient thoracic computed tomography scans and tested the effect of anterior vs. posterior DP locations on baseline impedance, myocardial power delivery, radiofrequency current path, and predicted lesion size.

## Results

For posterior left atrium ablation, the baseline impedance, total current delivered, current distribution, and proportion of power delivered to the myocardium were all similar with both anterior and posterior DP locations, resulting in similar RFCA lesion sizes (< 0.2 mm difference). For anterior right ventricular (RV) ablation, an anterior DP location resulted in slightly higher proportion of power delivered to the myocardium and lower baseline impedance leading to slightly larger RFCA lesions (0.6 mm deeper and 0.8 mm wider).

## Conclusions

An anterior vs. posterior DP location will not meaningfully affect RFCA for posterior left atrial ablation, and the slightly larger lesions predicted with anterior DP location for anterior RV ablation are of unclear clinical significance.

**Tweet:** Does the location of the dispersive patch affect RF lesion size? Can an anterior patch location lead to less oesophageal injury or better ablations? The answer depends on impedance.

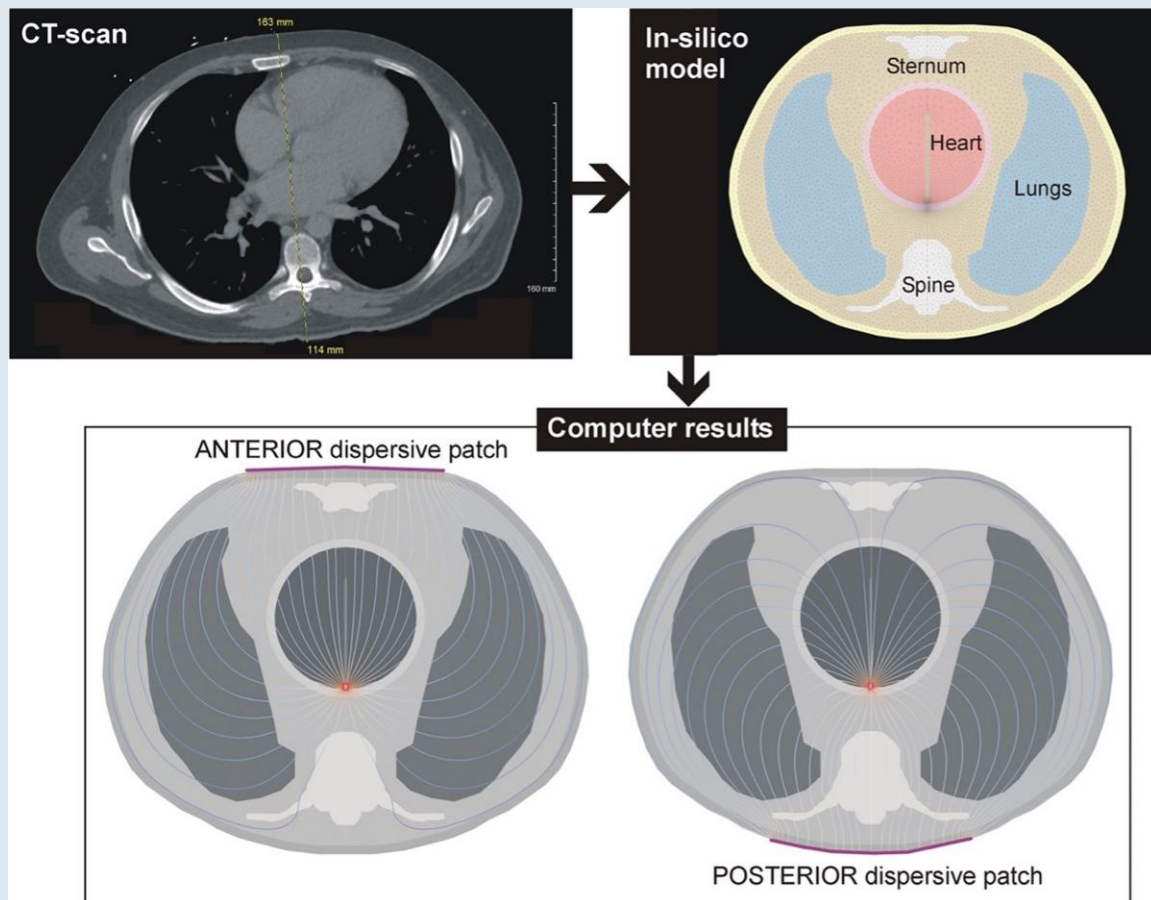
\* Corresponding author. Tel: +617 667 8800; fax: +617 632 7620. E-mail address: [adavila@bidmc.harvard.edu](mailto:adavila@bidmc.harvard.edu)

† The first two authors contributed equally to the work.

© The Author(s) 2023. Published by Oxford University Press on behalf of the European Society of Cardiology.

This is an Open Access article distributed under the terms of the Creative Commons Attribution-NonCommercial License (<https://creativecommons.org/licenses/by-nc/4.0/>), which permits non-commercial re-use, distribution, and reproduction in any medium, provided the original work is properly cited. For commercial re-use, please contact [journals.permissions@oup.com](mailto:journals.permissions@oup.com)

## Graphical Abstract



*In silico* model of radiofrequency ablation—Human thoracic computed tomography measurements allow the creation of realistic computer simulations of current delivery during ablation of different locations in the heart. Current distribution can be modelled to show differences in ablation with an anterior vs. posterior dispersive patch location.

## Keywords

Computer modelling • Dispersive patch • *In silico* model • Radiofrequency ablation

## What's new?

- Computer modelling based upon clinical computed tomography scans of the thorax suggests anterior location of the dispersive patch electrode during radiofrequency location does not affect current delivery and lesion size on the posterior left atrium compared to a more traditional posterior location. Moving the dispersive patch is unlikely to therefore prevent oesophageal injury.
- An anterior dispersive patch location may, however, slightly increase the size of lesions when ablation near anterior structures, such as right ventricular outflow tract ablation.
- Mechanistically, the differences in lesion sizes and power delivery between dispersive patch electrodes were driven by differences in baseline impedances.

## Introduction

Radiofrequency (RF) catheter ablation can successfully treat atrial and ventricular tachyarrhythmias.<sup>1,2</sup> Effective radiofrequency lesions require transmural or deep destruction of myocardial tissue. However, thermal energy delivery can

also create collateral tissue injury of nearby structures, including the oesophagus, phrenic nerve, normal conduction system, lung, and coronary vessels. In rare cases, RF energy delivery in the posterior left atrium (LA) can lead to an atrio-oesophageal fistula, which can be catastrophic and potentially lethal.

In other circumstances, however, current delivery to the local myocardium is insufficient to heat and destroy deep or intramural arrhythmia foci, which can then require for riskier forms of myocardial access or energy delivery for successful treatment such as epicardial or coronary vessel access, hybrid surgical access, bipolar ablation, coronary vessel alcohol injection, or hypotonic fluid irrigation.<sup>3-7</sup> Most RF catheter ablation (RFCA) procedures now use open-irrigated catheters and a power-controlled monopolar setup with current delivered from the catheter tip to adjacent myocardium and surrounding blood pool to generate resistive and conductive heating to destroy tissue and generate a large enough lesions to be effective. In the monopolar circuit, the remaining current returns to the RF generator through the body's tissues and a dispersive patch (DP) electrode. The proportion of current that enters the local myocardium for lesion formation is proportional to the power generated in the generator and the impedances of the catheter-myocardial interface and the rest of the organs between the catheter tip and the DP. The DP is most often placed on the skin on

**Table 1** Clinical data of the patients

Pt #	Sex	Age (years)	BMI (kg/m <sup>2</sup> )	BSA (m <sup>2</sup> )	Sternum-LA (mm)	LA-spine (mm)
1	M	33	34.18	2.41	163	114
2	M	58	39.38	2.27	159	139
3	F	38	37.73	2.37	170	110
4	M	84	29.52	1.87	142	105
5	F	43	30.30	1.68	149	89
6	M	61	26.41	1.94	140	109
7	F	90	25.06	1.73	140	114
8	M	55	36.24	2.58	171	125
9	M	67	29.40	2.14	161	160
10	M	72	34.96	2.49	161	128
11	M	66	29.98	2.02	174	129
12	F	61	24.80	1.82	137	112
13	M	73	26.66	2.17	165	106
14	F	49	35.48	1.96	146	113
15	M	75	22.96	2.01	149	100
16	M	86	31.48	2.05	146	117
17	M	59	30.78	2.24	171	134
18	M	79	30.72	2.09	168	127
19	M	69	37.31	2.50	172	155
20	F	63	17.38	1.37	110	73
<b>Mean</b>		<b>64.1</b>	<b>30.54</b>	<b>2.09</b>	<b>154.7</b>	<b>118.0</b>
<b>SD</b>		<b>15.5</b>	<b>5.59</b>	<b>0.31</b>	<b>16.2</b>	<b>20.4</b>

BMI, body mass index; F, female; LA, left atrium; M, male.

Bold signifies the summary rows of the table, which highlights that fact.

the patient's back, flanks, or thighs, with each location creating a different impedance due to different path lengths and different properties of intervening tissues, such as lung, bone, muscle, and fat.

The location and size of the DP may therefore be used to modulate the biophysics of RFCA and increase or decrease current delivery to local tissue as needed to create shallower lesions to avoid collateral tissue damage in some scenarios and create deeper, larger lesions to reach deep arrhythmia foci in others. Some groups have proposed that an anterior DP location may direct the current path away from posterior structures (such as the oesophagus) and towards anterior structures [such as right ventricular (RV) outflow tract tissue].<sup>8–12</sup> Computer modelling affords the opportunity to assess and control numerous variables to form predictions about complex biophysical systems, including RFCA.<sup>13,14</sup> The present study uses an *in silico* model of posterior LA and anterior RV RFCA to test the hypothesis that the DP location does not significantly affect the current distribution around the catheter tip during RFCA but may affect lesions size through differences in impedance due to factors far from the catheter tip, such as tissue composition and catheter tip-to-DP distance rather than redirecting the current itself.

## Methods

### Preliminary clinical study to estimate distance between ablation posterior left atrial wall electrode and dispersive patch

We conducted measurements on 20 consecutive patients of varying age, sex, and body mass index undergoing computed tomography of the thorax.

This study protocol was approved by the local institutional review board. We measured the distances sternum – LA wall (corresponding to an anterior position of the DP) and spine – LA (corresponding to a posterior position) for the atrial measurements. *Table 1* shows the measured distances and other biometric data. The distance to the anterior side ( $154.7 \pm 16.2$  mm) was significantly greater than to the posterior side ( $118.0 \pm 20.4$  mm;  $P < 0.001$ ). The mean distance between anterior and posterior position was approximately 272 mm. *Figure 1A* shows the computed tomography (CT) scan image of the patient #1. *Supplementary material* includes the CT scan slices of the 20 patients.

### Description of the *in silico* models

The *in silico* RFCA model solved for RF power deposition using Laplace's equation and thermal conduction using the Bioheat equation<sup>13</sup> to build 8400-element models and computed the initial impedance, percentages of power delivered to myocardium and blood, total RF current, and lesion size (using the 50°C isoline) after a 25 W —30 s ablation.

The model anatomic schema was derived from the CT scan of Patient #1 (*Figure 1A*) who had LA and anterior and posterior distances with values close to the sample mean. The model simulated RFCA of the posterior LA and was later modified to simulate RFCA in the anterior RV (to mimic ablation in the anterior RVOT). The model included bony structures (spine and sternum) and lungs, all surrounded by a 50% mix of muscle tissue and infiltrated fat (*Figure 1B*). An additional case was considered by assuming a greater amount of infiltrated fat (up to 80%) as suggested by the CT images. The heart was modelled as a sphere (10 cm inner diameter) full of blood with a shell mimicking the cardiac wall (thickness varying from 4 to 8 mm). Inside the cardiac chamber, an RF catheter was placed in perpendicular orientation on the posterior cardiac wall (with insertion depths of

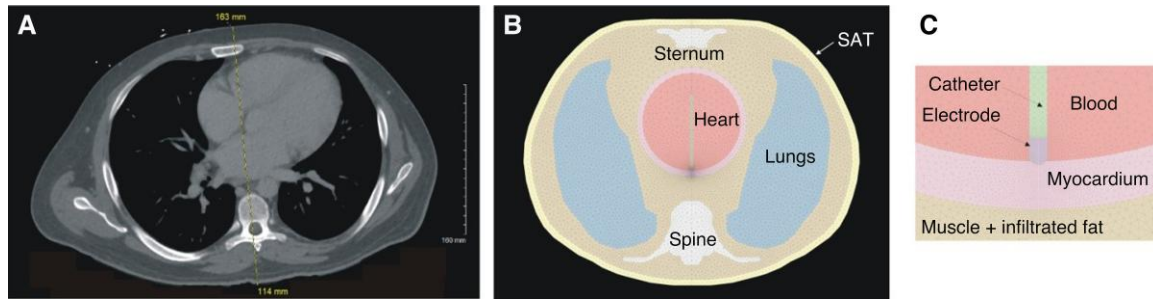


**Figure 1** (A) CT scan from patient #1. (B) Computer model (units in mm) of posterior LA RFCA inspired by the CT scan image and including the most representative organs. (C) Zoom of the RF catheter and cardiac wall. CT, computed tomography; LA, left atrium; RF, radiofrequency; RFCA, RF catheter ablation.

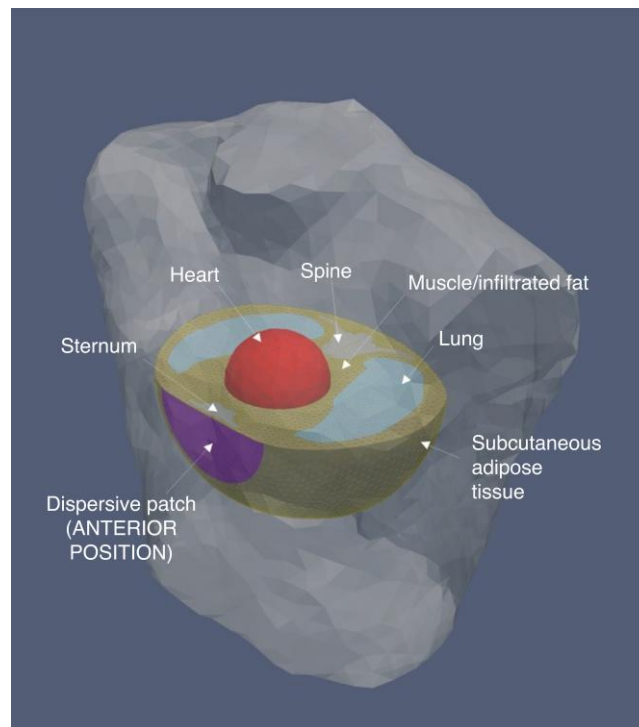


**Figure 2** Elements of the computational model and their relationship with the patient's torso for the case of the dispersive patch positioned on the anterior side.

0.3, 0.5, and 0.7 mm to model varying contact force) (see Figure 1C). The RF catheter comprised of a metal electrode (7Fr, 3.5 mm) and a fragment of plastic tubing. The electrode irrigation was modelled by fixing a value of 45° C in the cylindrical zone of the electrode tip and leaving the semi-spherical tip free, mimicking a multi-hole electrode assuming that irrigation occupies almost the entire surface of the electrode.<sup>14</sup>

To aid in computation, the model was two dimensional with axial symmetry, which implies that the volumes corresponding to the organs are created by rotation around the axis of the RF catheter, as illustrated in Figure 2. To keep the axial symmetry, DP was assumed to be a 7-cm radius disk, with a contact area of 154 cm<sup>2</sup> (which is a value very similar to the commercially available DPs and would allow symmetry to simplify the calculations).

For the LA RFCA simulations, the heart was placed so that the distances between the electrode and the posterior and anterior part were 117 and 154 mm, respectively, corresponding to the mean values measured in the patient sample (Table 1). Additional simulations were conducted modifying these distances  $\pm 20$  mm given the standard deviation of the clinical measurements. Although the total distance between anterior and posterior sides can vary significantly based on patient body size, it was kept constant at 272 mm to assess the impact of the distance between ablation target location and DP. To test the effect of varying LA position relative to anterior or posterior DPs, we considered three different locations of LA respect to the posterior and anterior sides: (i) LA relatively centred with respect to the anterior and posterior sides (similar to that observed in Patient #9), (ii) mean distances to the anterior and posterior sides (similar to that observed

**Table 2** Baseline impedance ( $Z$ ), percentage of power targeted to the posterior LA myocardium ( $P_M$ ), and total current ( $I$ ) computed for anterior and posterior position of the dispersive patch

	Posterior			Anterior		
	$Z$ ( $\Omega$ )	$P_M$ (%)	$I$ (mA)	$Z$ ( $\Omega$ )	$P_M$ (%)	$I$ (mA)
Patient #9	121.6 $\pm$ 1.8	11.4 $\pm$ 1.3	457 $\pm$ 2	115.2 $\pm$ 1.7	12.0 $\pm$ 1.4	470 $\pm$ 6
Patient #1	120.3 $\pm$ 1.8	11.6 $\pm$ 1.3	460 $\pm$ 2	117.1 $\pm$ 1.7	11.8 $\pm$ 1.3	467 $\pm$ 2
Patient #13	119.4 $\pm$ 1.8	11.5 $\pm$ 1.3	462 $\pm$ 2	119.6 $\pm$ 1.7	11.4 $\pm$ 1.3	461 $\pm$ 2

LA, left atrium.

**Table 3** Left atrium lesion sizes computed (in mm) for anterior and posterior position of the dispersive patch

	Posterior			Anterior		
	MW	SW	D	MW	SW	D
Patient #9	8.7 $\pm$ 0.4	6.1 $\pm$ 0.2	5.3 $\pm$ 0.3	8.9 $\pm$ 0.4	6.2 $\pm$ 0.2	5.3 $\pm$ 0.3
Patient #1	8.7 $\pm$ 0.4	6.1 $\pm$ 0.2	5.3 $\pm$ 0.3	8.8 $\pm$ 0.4	6.2 $\pm$ 0.2	5.3 $\pm$ 0.3
Patient #13	8.6 $\pm$ 0.4	6.1 $\pm$ 0.2	5.1 $\pm$ 0.3	8.6 $\pm$ 0.4	6.1 $\pm$ 0.2	5.0 $\pm$ 0.3

D, maximum depth; MW, maximum width; SW, surface width.

in Patient #1), and (iii) LA located only 97 mm from the posterior (similar to that observed in Patient #13). These three cases were chosen to represent the boundary conditions for the model. The electrical and thermal properties of the tissues were taken from the IT'IS Foundation database<sup>15</sup> while the ablation catheter properties were taken from Pérez *et al.*<sup>16</sup>

Supplementary material online, Table S1 shows the characteristics of the materials used in the model. The values for lung were the mean between inflated and deflated. The values for bone (spine and sternum) were the mean between cortical and trabecular bone. The values for the tissue surrounding organs were the mean between muscle and subcutaneous fat. The 6 mm outer layer was assumed to be subcutaneous adipose tissue (SAT, Figure 1B).

Remote factors, such as the amount of SAT underneath the DP, may affect the baseline impedance and hence the lesion size.<sup>12,17</sup> There are no conclusive data about differences of subcutaneous fat in anterior and posterior side. For instance, Störchle *et al.*<sup>18</sup> found a difference of 3 mm greater thickness of anterior fat compared to posterior fat above fibrous septae. While this superficial layer is quite compact and exhibits stable thickness, the deep layer consists of large lobules of fat and varies in thickness in different regions of body and may contribute more to baseline impedance differences.<sup>19</sup> We used the computational model to study how the greater accumulation of fat on the posterior or anterior side could modify the results by increasing the thickness of the outer layer by 4 mm, i.e. from 6 to 10 mm, just below each DP position.

We next adapted the model to mimic an RF ablation of arrhythmia originating from the anterior RV outflow tract (RVOT), where the RF electrode is positioned closer to the sternum. In this case, the catheter was in contact with the anterior wall of the sphere that simulates the heart (a 4 mm cardiac thickness was considered here given the thinner RV tissue at this location) at three insertion depths (0.3, 0.5, and 0.7 mm).

## Statistics

This study used a physics-based mechanistic model. We assumed an uncertainty in the LA and anterior and posterior distances, the ratio between skeletal muscle and fat in the tissues surrounding the organs (50% and 80%), cardiac wall thickness (4–8 mm), and insertion depths of electrode (0.3–0.7 mm). The Excel file (see Supplementary material) includes all case

permutations with regard to the above variables (114 full separate simulations). This provided 54 unique cases as a representative sample of RFCA of LA under varying conditions. Three additional cases were considered to study the case of RV ablation. The comparison of results between DP positions was performed using the paired t-test. Statistical significance was assumed when the  $P$ -value ( $P$ ) was lower than 0.05.

## Results

### Posterior left atrial wall ablation

Table 2 shows the electrical results parameters for both positions of DP and for the three patient models. For each patient model, nine simulations were conducted by changing the cardiac wall thickness (4, 6, and 8 mm) and insertion depth of the electrode (0.3, 0.5, and 0.7 mm). Table 2 shows the mean and standard deviation of these nine simulations. The baseline impedance was higher with posterior position ( $P < 0.001$ ), specifically by 6.4, 3.2, and 0.15  $\Omega$  in patients #9, #1, and #13, respectively. Both the percentages of power targeted to the myocardium and total current delivered were higher with anterior position ( $P < 0.001$ ), but the differences were small: less than 0.6% and 13 mA, respectively.

Table 3 shows the lesion sizes for both positions of DP and for the three patient models. The LA lesions were wider with anterior position ( $P < 0.001$ ), with differences always smaller than 0.2 mm, while there were no significant differences in the lesion depth ( $P = 0.85$ ). Figure 3 shows an overview of the distribution of the electric field lines along the entire torso section, illustrating the path followed by RF current from the ablation electrode (located on the endocardium on the posterior wall) to the DP. RF current around the ablation electrode follows an almost identical path regardless of the DP position. Figure 4 shows the temperature and voltage distributions, along with electric field lines around the ablation electrode for the two DP positions. Similar to the data shown in Table 3, the LA lesion sizes were almost identical for both positions, both in depth and maximum and surface widths. Although these plots correspond with a specific case (Patient #1, 6 mm cardiac

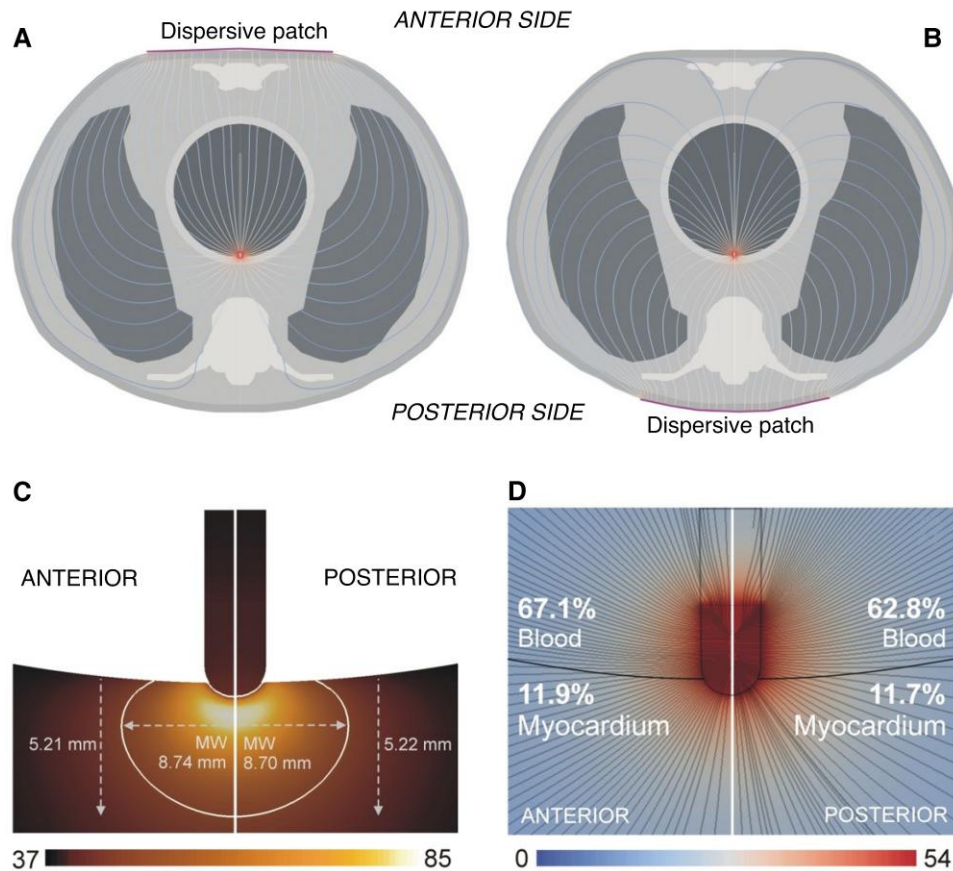


**Figure 3** Electric field lines for anterior (A) and posterior (B) positions of the dispersive patch in the case of RF ablation on the posterior LA wall. The plots correspond with the Patient #1 (6 mm cardiac wall, 0.5 mm insertion depth). (C) Temperature distributions (in °C) for anterior and posterior positions of the dispersive patch in the case of RF ablation on the posterior LA wall. Solid white line represents the lesion boundary (MW: maximum width). (D) Voltage distributions (in V) around the RF electrode (in colour) and electric field lines (black) for anterior and posterior positions. The values correspond with the percentages of power targeted to myocardium and blood in each case. The plots correspond with the Patient #1 (6 mm cardiac wall, 0.5 mm insertion depth). RF, radiofrequency; LA, left atrium.

wall and 0.5 mm insertion depth), the trends are representative of all cases.

When the model corresponding with Patient #1 was modified by increasing the thickness of the SAT from 6 to 10 mm the baseline impedance was higher with posterior position ( $122.5 \pm 2.8$  vs.  $119.1 \pm 2.7 \Omega$ ,  $P = 0.005$ ). The LA lesions were wider with anterior position ( $P < 0.001$ ), with differences always smaller than 0.04 mm, while there were no significant differences in the lesion depth ( $P = 0.82$ ). Finally, when the tissue surrounding the organs was considered 30% fattier (mix of 80% fat and 20% muscle, instead of 50%–50%), the baseline impedance was higher with posterior position ( $131.2 \pm 2.0$  vs.  $128.1 \pm 2.0 \Omega$ ,  $P < 0.005$ ), and the LA lesions were significantly wider ( $P < 0.001$ ) and deeper ( $P = 0.003$ ) with anterior position, with differences always smaller than 0.05 and 0.01 mm, respectively.

### Right ventricular outflow tract ablation

Graphical abstract shows an overview of the distribution of the electric field lines along the entire torso section in the case of ablation electrode located on the anterior wall, i.e. mimicking RF ablation at RVOT. In the case of a posterior DP, there is a slightly greater amount of RF current flowing through the blood pool which creates a relatively higher

percentage of power targeted to the myocardium in the case of anterior DP: 11.3 vs. 9.6%,  $P = 0.002$  (Figure 4B). The anterior position implied a baseline impedance 17  $\Omega$  lower than the posterior position ( $P < 0.001$ ), which resulted in a higher current (481 vs. 446 mA,  $P < 0.001$ ). These differences in electrical terms, although small, resulted in a slightly larger lesion in the case of the anterior DP ( $P < 0.001$ ), ~0.4 mm deeper and ~0.8 mm wider (Figure 4A).

### Discussion

In this study an *in silico* model of RFCA was developed to explore the effect of the distance between the ablation electrode and DP on baseline impedance and lesion formation. A diverse set of real patient anatomic features were incorporated into the model to generate applicable results to clinical practice. The key findings of this study are as follows:

- (1) The posterior DP location was associated with a slightly higher baseline impedance in the posterior LA and moderately higher baseline impedance in the anterior RV compared to an anterior DP location.
- (2) For posterior LA RFCA, the percentage of power deposited to myocardium by the ablation electrode and ablation sizes were statistically

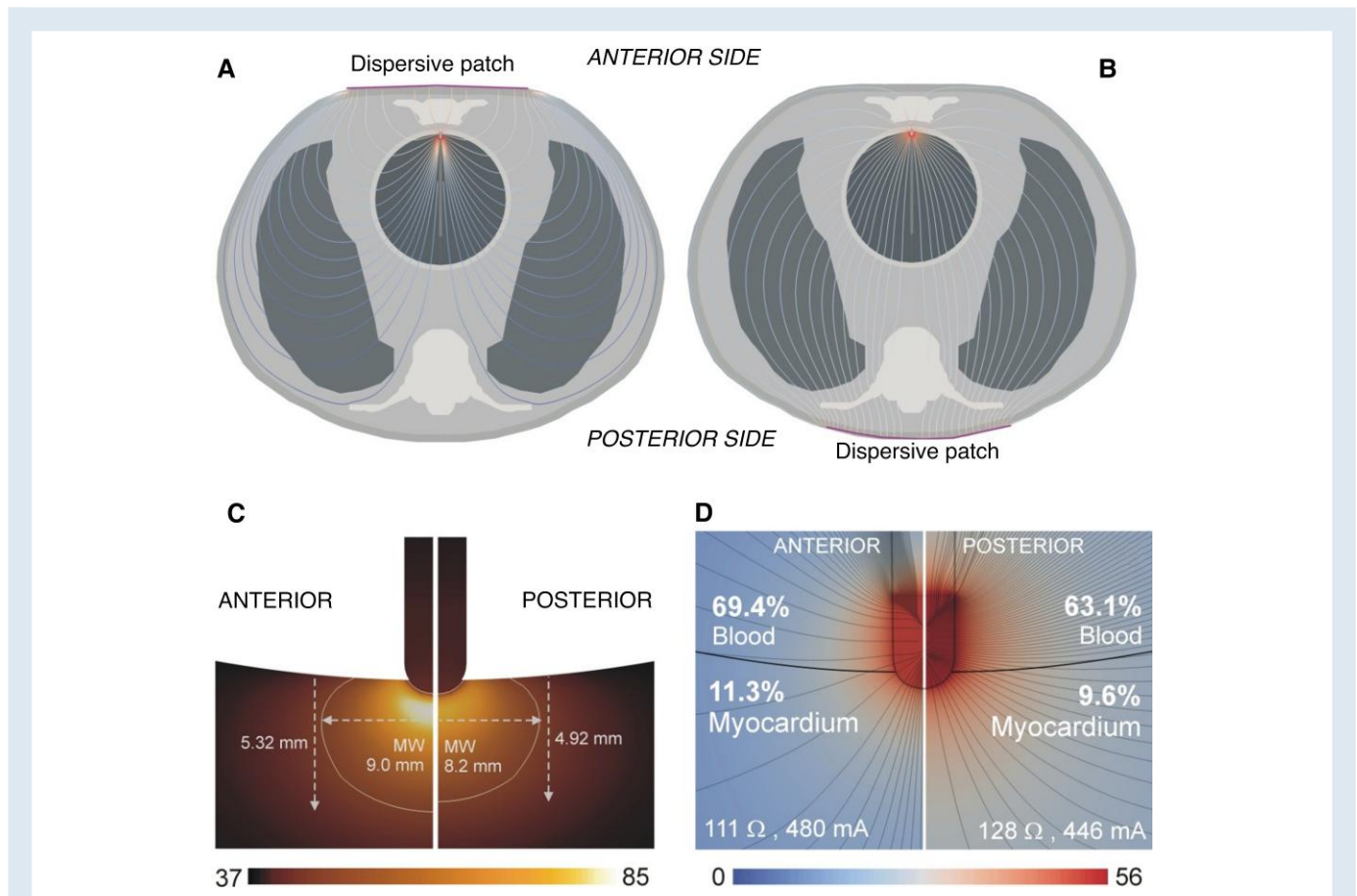


**Figure 4** Electric field lines for anterior (A) and posterior (B) positions of the dispersive patch in the case of RF ablation on the anterior cardiac wall. The plots correspond with the Patient #9 (4 mm cardiac wall, 0.5 mm insertion depth). (C) Temperature distributions (in °C) for anterior and posterior positions of the dispersive patch in the case of RF ablation on the anterior cardiac wall. Solid white line represents the lesion boundary (MWV: maximum width). (D) Voltage distributions (in V) around the RF electrode (in colour) and electric field lines (black) for anterior and posterior positions. The values correspond with the percentages of power targeted to myocardium and blood in each case. The plots correspond with the Patient #9 (4 mm cardiac wall, 0.5 mm insertion depth). RF, radiofrequency.

- but not clinically significantly different with an anterior vs. posterior DP location.
- (3) For posterior LA RFCA, RF current around the ablation electrode follows an almost identical path regardless of the DP position, suggesting there is no redirection of current based on the DP location.
  - (4) In contrast, for anterior RV ablation, the model suggests slightly more power will be deposited in the myocardium with the anterior DP which results in lesions approximately 0.4 mm deeper and 0.8 mm wider than the posterior position. This is due to more current going through the blood pool with the posterior DP and the slightly higher baseline impedance with the posterior DP location.
  - (5) With increasing SAT thickness or increased fat content of soft tissues, the baseline impedance increased but the RFCA lesion size remained nearly the same in both DP locations for posterior LA ablation.

Preclinical RFCA models have demonstrated that baseline impedance is negatively correlated with current and therefore lesion size.<sup>12</sup> Prior clinical studies have suggested reducing baseline impedance can improve current delivery during RFCA by changing the location or number of dispersive electrodes, which may facilitate successful ablation in intramural ventricular substrates.<sup>17</sup> While most electrophysiology laboratories place the DP on the patient's back, flanks, or thigh, some groups have advocated placing the DP anteriorly on the chest.

A recent pilot study compared the anterior and posterior positions of the DP during AF ablation.<sup>8</sup> Despite the very small sample size (64 patients), the authors found a significant difference between baseline impedance in anterior vs. posterior DP positions ( $134 \pm 7$  vs.  $122 \pm 8$  Ω). Although they found no significant difference in AF recurrence rate during one-year follow up, they suggested that anterior DP might (i) redirect RF current away from the oesophagus to improve the procedural safety and (ii) act as an additional protection given higher impedance values would reduce the energy delivered to the tissue.

The concept of 'redirecting RF current' had been already proposed by the same group in a 2017 case report describing the successful ablation of a RVOT ventricular arrhythmia.<sup>9</sup> To our knowledge, there are very few studies addressing this issue. The pilot study by Nath *et al.*<sup>10</sup> on 20 patients reported no differences in impedance between interscapular and left thigh positions, while Jain *et al.*<sup>11</sup> did find significant differences in lesion size (but not in impedance values) using an *in vivo* experimental model in which two DP positions were compared: opposite vs. frontal the catheter tip.

The results presented here suggest minimal difference in lesion formation would be expected during RFCA of the posterior LA wall (which is where ablation can lead to the risk of oesophageal injury during the ablation of atrial fibrillation) simply by moving the DP to an anterior location with all other parameters being equal. Given the small

differences in impedance, essentially equivalent proportion power delivered, and similar RF current path, improving the safety and effectiveness of RFCA lesion formation should focus on other biophysical factors including modulating RF power, lesion time, contact force, and baseline impedance.

The posterior LA, however, is located nearly in the middle of the thorax anteroposterior dimension. Much larger relative differences in distances from the ablation catheter tip to each DP location are seen in anterior cardiac structures, such as the RVOT. In the case of RFCA in the anterior RV, which is performed during ablation of RVOT ventricular tachycardia or premature ventricular contractions, an anterior DP location may create slightly larger lesions based on our model due to altered current paths and lower system impedance with an anterior DP position. Futyma *et al.*<sup>9</sup> described a case with the use of an anterior DP location allowed the successful ablation of an anterior RVOT premature ventricular contraction focus that was refractory to RFCA with a posterior DP. However, given the thickness of the RVOT is only 3–6 mm,<sup>20</sup> the modest additional lesion depth with the anterior DP is of uncertain clinical significance in terms of increasing ablation efficacy. This lesion size difference could be achieved without switching DP location by cautiously increasing RFCA power, delivering longer lesions, or reducing baseline impedance by adding an additional DP.

Our model's results did not reproduce the trend found by Futyma *et al.*<sup>8</sup> regarding a higher baseline impedance (~12  $\Omega$ ) when the DP is positioned on the anterior side. In contrast, we observed a tendency to higher values (up to 8  $\Omega$ ) with a posterior DP position during posterior LA RFCA. While DP position itself may not significantly change lesion formation in the LA, other tissue characteristics in the current path may play a role.<sup>21</sup> When the fat content of the tissue surrounding the organs was changed from 50% to 80%, baseline impedance increases from ~120 to ~130  $\Omega$ , making the lesion 0.5–0.8 smaller.

However, the increased lesion depth of 0.6 mm could likely be achieved without switching DP location by cautiously increasing RFCA power, delivering longer lesions, or reducing baseline impedance by adding an additional DP.

A limitation of this study is that it is based on a specific geometry inspired by the images of a representative patient. Despite this, the model includes all the relevant organs in terms of size, electrical and thermal properties, and proximity to the ablation electrode, which makes it possible to reproduce the electrical and thermal phenomena involved in RFCA. Even despite having worked with a 2D model based on rotational symmetry, there are no physical reasons to think that the trends regarding the effect of DP position (anterior vs. posterior) on the RF current around the ablation electrode and the lesion size are different if a more realistic 3D model including more organs is considered. It is important to note that this model does not account for variations in DP geometry and materials between manufactures, quality of contact, or number of DPs used. However, the purpose of the study was to test the specific hypothesis regarding distance of the DP to the site of ablation, and only computer simulation allows isolating and varying specific variables in an unconfounded way to help elucidate a physical concept.

## Conclusions

Our results suggest that the position of the DP (anterior or posterior) does not redirect the RF current towards that position. The spatial distribution of RF currents around the ablation electrode is not significantly altered by where the DP is positioned during posterior LA ablation. There is also no clinically significant impact on the percentage of power targeted to the myocardium, resulting in minimal difference in lesion size. With anterior RV ablation, however, an anterior DP location creates slightly deeper and wider lesions due to lower baseline impedance leading to higher percentage of the power being delivered to the

myocardium. Preclinical and human studies assessing the safety and efficacy of changing DP location are needed to confirm these results.

## Supplementary material

Supplementary material is available at *Europace* online.

## Funding

This study was supported by Spanish MCIN/AEI/10.13039/501100011033 (E.B.; Grant RTI2018-094357-B-C21), 'Agencia Nacional de Promoción Científica y Tecnológica de Argentina' (R.I.; PICT-2016-2303), and Programa de Becas Externas Postdoctorales para Jóvenes Investigadores del CONICET (R.I.).

**Conflict of interest:** None declared.

## Data availability

The data underlying this article will be shared on reasonable request to the corresponding author.

## References

- Cronin EM, Bogun FM, Maury P, Peichl P, Chen M, Namboodiri N *et al.* 2019 HRS/EHRA/APHS/LAHS expert consensus statement on catheter ablation of ventricular arrhythmias. *Heart Rhythm* 2020;**17**:e2–e154.
- Calkins H, Hindricks G, Cappato R, Kim YH, Saad EB, Aguinaga L *et al.* Document reviewers: 2017 HRS/EHRA/ECAS/APHS/SOLAECE expert consensus statement on catheter and surgical ablation of atrial fibrillation. *Europace* 2018;**20**:e1–e160.
- Cardoso R, Assis FR, D'Avila A. Endo-epicardial vs endocardial-only catheter ablation of ventricular tachycardia: a meta-analysis. *J Cardiovasc Electrophysiol* 2019;**30**:1537–48.
- Soejima K, Couper G, Cooper JM, Sapp JL, Epstein LM, Stevenson WG. Subxiphoid surgical approach for epicardial catheter-based mapping and ablation in patients with prior cardiac surgery or difficult pericardial access. *Circulation* 2004;**110**:1197–201.
- Nguyen DT, Tzou WS, Sandhu A, Gianni C, Anter E, Tung R *et al.* Prospective multicenter experience with cooled radiofrequency ablation using high impedance irrigant to target deep myocardial substrate refractory to standard ablation. *JACC Clin Electrophysiol* 2018;**4**:1176–85.
- Koruth JS, Dukkupati S, Miller MA, Neuzil P, d'Avila A, Reddy VY. Bipolar irrigated radiofrequency ablation: a therapeutic option for refractory intramural atrial and ventricular tachycardia circuits. *Heart Rhythm* 2012;**9**:1932–41.
- Kreidieh B, Rodríguez-Mañero M, Schurmann P, Ibarra-Cortez SH, Dave AS, Valderrábano M. Retrograde coronary venous ethanol infusion for ablation of refractory ventricular tachycardia. *Circ Arrhythm Electrophysiol* 2016;**9**:10.1161/CIRCEP.116.004352 e004352.
- Futyma P, Burda N, Surowiec A, Kogut A, Iwanski M, Swierczek P *et al.* Anterior position of dispersive patch for esophageal protection during atrial fibrillation ablation. A pilot feasibility study. *Europace* 2021;**23**(Supplement ): iii264.
- Futyma P, Kułakowski P. Frontal placement of dispersive patch for effective ablation of arrhythmia originating from the anterior right ventricular outflow tract. *J Interv Card Electrophysiol* 2007;**49**:327.
- Nath S, DiMarco JP, Gallop RG, McRury ID, Haines DE. Effects of dispersive electrode position and surface area on electrical parameters and temperature during radiofrequency catheter ablation. *Am J Cardiol* 1996;**77**:765–7.
- Jain MK, Tomassoni G, Riley RE, Wolf PD. Effect of skin electrode location on radiofrequency ablation lesions: an in vivo and a three-dimensional finite element study. *J Cardiovasc Electrophysiol* 1998;**9**:1325–35.
- Barkagan M, Rottmann M, Leshem E, Shen C, Buxton AE, Anter E. Effect of baseline impedance on ablation lesion dimensions: a multimodality concept validation from physics to clinical experience. *Circ Arrhythm Electrophysiol* 2018;**11**:e006690.
- González-Suárez A, Pérez JJ, Irastorza RM, D'Avila A, Berjano E. Computer modeling of radiofrequency cardiac ablation: 30 years of bioengineering research. *Comput Methods Programs Biomed* 2022;**214**:106546.
- Pérez JJ, González-Suárez A, Maher T, Nakagawa H, d'Avila A, Berjano E. Relationship between luminal esophageal temperature and volume of esophageal injury during RF ablation: in silico study comparing low power-moderate duration vs. High power-short duration. *J Cardiovasc Electrophysiol* 2022;**33**:220–30.
- Hasgall PA, Di Gennaro F, Baumgartner C, Neufeld E, Lloyd B, Gosselin MC *et al.* *ITIS Database for Thermal and Electromagnetic Parameters of Biological Tissues*, Version 4.1, Feb 22, 2022. [itis.swiss/databse](https://www.itis.swiss/databse) (2 October 2022, date last accessed).



16. Pérez JJ, Ewertowska E, Berjano E. Computer modeling for radiofrequency bipolar ablation inside ducts and vessels: relation between pullback speed and impedance progress. *Lasers Surg Med* 2020;**52**:897–906.
17. Shapira-Daniels A, Barkagan M, Rottmann M, Sroubek J, Tugal D, Carlozzi MA et al. Modulating the baseline impedance: an adjunctive technique for maximizing radiofrequency lesion dimensions in deep and intramural ventricular substrate: an adjunctive technique for maximizing radiofrequency lesion dimensions in deep and intramural ventricular substrate. *Circ Arrhythm Electrophysiol* 2019;**12**:e007336.
18. Störchle P, Müller W, Sengeis M, Lackner S, Holasek S, Fürhapter-Rieger A. Measurement of mean subcutaneous fat thickness: eight standardised ultrasound sites compared to 216 randomly selected sites. *Sci Rep* 2018;**8**:16268.
19. Markman B, Barton EF Jr. Anatomy of the subcutaneous tissue of the trunk and lower extremity. *Plast Reconstr Surg* 1987;**80**:248–54.
20. Issa ZF, Miller JM, Zipes DP. Chapter 23—adenosine-sensitive (outflow tract) ventricular tachycardia. In Issa ZF, Miller JM, Zipes DP (eds), *Clinical Arrhythmology and Electrophysiology: A Companion to Braunwald's Heart Disease*. 2nd ed. Philadelphia, PA: W.B. Saunders; 2012. p562–86. ISBN 9781455712748, <https://doi.org/10.1016/B978-1-4557-1274-8.00023-3>.
21. Irastorza RM, Maher T, Barkagan M, Liubasuskas R, Pérez JJ, Berjano E et al. Limitations of baseline impedance, impedance drop and current for radiofrequency catheter ablation monitoring: insights from in silico modeling. *J Cardiovasc Dev Dis* 2022;**9**:336.